



HAL
open science

Modelling of heat transfer within heterogeneous media by Brownian walkers

Vincent Gonneau, Denis Rochais, Franck Enguehard

► **To cite this version:**

Vincent Gonneau, Denis Rochais, Franck Enguehard. Modelling of heat transfer within heterogeneous media by Brownian walkers. *International Journal of Heat and Mass Transfer*, 2022, 184, pp.122261. <10.1016/j.ijheatmasstransfer.2021.122261>. <hal-03844843>

HAL Id: hal-03844843

<https://hal.science/hal-03844843v1>

Submitted on 8 Jan 2024

HAL is a multi-disciplinary open access archive for the deposit and dissemination of scientific research documents, whether they are published or not. The documents may come from teaching and research institutions in France or abroad, or from public or private research centers.

L'archive ouverte pluridisciplinaire HAL, est destinée au dépôt et à la diffusion de documents scientifiques de niveau recherche, publiés ou non, émanant des établissements d'enseignement et de recherche français ou étrangers, des laboratoires publics ou privés.



Distributed under a Creative Commons CC BY-NC 4.0 - Attribution - Non-commercial use - International License

Modelling of heat transfer within heterogeneous media by Brownian walkers

Vincent Gonneau^{1*}, Denis Rochais¹, Franck Enguehard²

¹ *CEA, DAM, Le Ripault, F-37260 Monts, France*

² *Institut Pprime, CNRS, Université de Poitiers, ISAE-ENSMA,
F-86962 Futuroscope Chasseneuil, France*

Abstract:

This work concerns the modelling of transient thermal conduction within a heterogeneous medium by the movement of Brownian walkers. The material structure is voxelized, and each walker transports an elementary enthalpy during its displacement within the structure. This enthalpy transport represents the conductive flow and makes it possible to simulate the conduction in a transient state with a quantitative stochastic approach. A study of the impact of the value of the time step is carried out to fix the choice conditions of this parameter, in particular in the presence of strong contrasts in thermophysical properties, and as such to define a validity framework of the diffusion model. Then several academic problems related to the behaviour of walkers are resolved in order to be able to account for different thermal solicitations and conditions at the boundaries (Dirichlet, Neumann, Newton) with Brownian walkers. These results have in particular made it possible to reproduce the so-called “rear face flash” experimental technique using a model by Brownian walkers over a homogeneous medium. Then, a stochastic transmission criterion based on the thermal effusivities is demonstrated to treat the meeting of a walker with an interface between two constituents within a heterogeneous medium. This work, focused on the mastery of the dynamics of Brownian walkers within heterogeneous media for the correct simulation of transient conduction, is a first step towards the modelling of the transient conduction-radiation coupling by means of Brownian walkers coupled to ray tracing techniques at the local scale of a voxelized structure.

Keywords: transient heat transfer, heat conduction, Brownian walkers, heterogeneous media, voxelized representation

*: corresponding author: vincent.gonneau93@gmail.com

Nomenclature

a	Thermal diffusivity ($\text{m}^2.\text{s}^{-1}$)	ΔV	Volume element (m^3)
\vec{B}	Vector representing the Brownian movement (-)	δh	Elementary enthalpy (J)
Bi	Biot number (-)	δt	Time step of the simulation (s)
C_p	Specific heat ($\text{J}.\text{kg}^{-1}.\text{K}^{-1}$)	$\overrightarrow{\delta X}$	Elementary displacement of a walker during a time step (m)
e	Thermal effusivity ($\text{J}.\text{K}^{-1}.\text{m}^{-2}.\text{s}^{-1/2}$)	δx	Spatial discretization (m)
H	Enthalpy (J)	ε	Very short length compared to δx (m)
h	Convective heat transfer coefficient ($\text{W}.\text{m}^{-2}.\text{K}^{-1}$)	η	Standard deviation (m)
L	Length of the medium (m)	λ	Thermal conductivity ($\text{W}.\text{m}^{-1}.\text{K}^{-1}$)
l	Entry length of a walker in the case of an imposed surface heat flux (m)	ρ	Density ($\text{kg}.\text{m}^{-3}$)
M	Number of walkers (-)	φ	Surface heat flux ($\text{W}.\text{m}^{-2}$)
m	Index of the constituent of the voxel (-)	$-^*$	Dimensionless quantity (-)
\mathcal{N}	Normal distribution (-)	$-_c$	Characteristic
N	Total number of voxels (-)	$-_{conv}$	Convective
n	Index of the position of the voxel (-)	$-_{eff}$	Effective
\mathcal{P}	Transmission criterion of a walker (-)	$-_f$	Final
r	Uniform random number $\in]0 ; 1[$ (-)	$-_{fl}$	Fluid
S	Surface (m^2)	$-_i$	Initial
T	Temperature (K)	$-_m$	Related to constituent m
t	Instant (s)	$-_n$	Related to voxel n
t_{pulse}	Pulse duration of the flash source (s)	$-_r$	Reference
V_v	Volume of a voxel (m^3)	$-_s$	Surface
x	Position in space of a walker (m)	$-_{so}$	Solid
α	Ratio of the characteristic diffusion length to the spatial discretization (-)	$-_{tr}$	Transmitted
ΔT	Temperature difference (K)		

1. Introduction

In many industrial applications, heterogeneous media like composite (fiber / resin) structures, cellular materials (ceramic, metallic or carbon foams) or refractory ceramics (fibrous media) are used to take advantage of their specific properties. These heterogeneous materials can be used as gas diffusers, solar energy volumetric receivers [1], heat exchangers [2] or as thermal insulators at high temperatures ($> 1800\text{K}$) [3]. In all these applications, seeking to improve their performances is continuous and entails a better understanding of the way heat circulates within these materials. Depending on their constitution and their operating temperature [4], the heat transfer within such media can be based more or less on radiation. In order to numerically predict their thermal behaviours over time, it is thus necessary to model the heat transfer by treating the conduction-radiation coupling. The study of the behaviour and of the conduction-radiation heat transfer within heterogeneous media is generally carried out according to two distinct approaches: the so-called continuous scale approach or an approach solving the equations at the local scale. The continuous scale approach is based on the principle of homogenisation of the thermal problem treated: the heterogeneous structure is replaced with an equivalent homogeneous medium. This approach has the advantage of being able to easily access the thermal behaviour of the material at the macroscopic scale and requires few computing resources (quantity of memory and calculation time). However the effective thermal properties, possibly anisotropic, of a heterogeneous material depend highly on the microstructural characteristics and the singularities present at this scale. In the case of a fibrous medium for example, the effective thermal properties and the thermal behaviour depend on the material that constitutes the fibres, their orientation, their distribution in space, their possible anisotropy and the quality of the contact between them. Consequently, the precise study of the thermal behaviour of the material, with an objective of improving its performance, requires setting up a so-called discrete approach by resolving the equations at the local scale of a numerical microstructure.

For a few decades now, many approaches developed in the heat transfer community aim to identify the thermophysical [5,6,7,8] and radiative [9,10,11] properties and to globally understand the thermal behaviour of heterogeneous materials based on numerical representations of their microstructures. The modelling of the different heat transfer modes and in particular of radiation at the local scale is made extremely complex when taking into account the microstructure of these materials (morphology, cohabitation of several phases that can be semi-transparent, anisotropic behaviour of the constituents). The study of heterogeneous media requires working on structures that are sufficiently large to be considered as Representative Elementary Volumes (REV) of the medium. Many deterministic numerical methods have been developed to attempt to best approach the exact solution of the Radiative Transfer Equation (RTE) and as such model the radiation as

precisely as possible in these complex media (P_n method [12], two flux method [13], discrete ordinates method [14,15,16]). These deterministic resolution methods require solving a linear system (for a given temperature field) where the number of unknowns is roughly proportional to the number of dimensions of the problem and to the fineness of the spatial discretization mesh [17]. The necessity of working on a REV, associated with the microstructural complexity of the medium, imposes a highly refined mesh, which can make it difficult to use these methods to locally model the heat transfer and in particular radiation.

The exponential progress in computing power in the last years has allowed for the development of stochastic techniques that are able to model the thermal phenomena by taking account of the increasingly complex microstructures of the media, the natures of the phases and the influence of the temperature. These techniques are based on the repetition of random and independent simulations within a calculation volume to model a physical problem. They are commonly referred to as Monte Carlo methods, and generally involve the motions of carriers according to specific statistical laws, either over a specified grid within the volume (these techniques are called Lattice Monte Carlo methods [18,19]) or over the entire volume. In particular, Monte Carlo methods in the form of random walks are developed to model the conduction-radiation coupling and to estimate the total thermal conductivity of fibrous composite materials [20] or open foams (Si-SiC) [6]. The “conductive walkers” in the opaque and grey conductive solid phase follow the Brownian movement while the “radiative walkers” are packets of photons moving at an infinite speed solely in the transparent (void) phase. This method is of real interest because it makes it possible to model a strong coupling at the local scale between the two transfer modes by using Monte Carlo techniques. However, it is still based on certain restrictive assumptions. First of all, the thermal radiation term is linearized, which is debatable at very high temperatures ($> 1800\text{K}$). Then, radiation is not resolved within the solid phase considered opaque. Likewise, conduction is not considered in the transparent phase. The coupled heat transfer is therefore not resolved in the volume in the microstructure but solely at the interfaces between the phases.

An entirely stochastic approach of the conduction-radiation coupling within heterogeneous media was initiated by Dauvois [21] over a numerically generated fibrous sample. In this work, the coupling was treated only in the fibre phase (assumed absorbing and non-scattering), conduction being ignored in the fluid phase (transparent gas or vacuum). Moreover, only in the steady state solution was looked for. Yet, important thermal gradients can take place within these materials during rapid transient states, which can result in substantial thermomechanical stresses applied to the materials. Advanced modelling of the coupled heat transfer within all of the phases in the transient state is therefore essential for knowledge of the behaviour of the material and for evaluating its performance.

This article discusses these modelling objectives by means of stochastic processes and focusses on the study of unsteady heat conduction within heterogeneous media. In this work, we will concentrate on the development and the validation of theoretical concepts that allow for the stochastic modelling of thermal diffusion. Section 2 will present these theoretical concepts allowing for modelling in particular different boundary conditions by means of Brownian walkers. The procedure treating heterogeneity and its impact on the travel of the walkers will then be demonstrated and validated in Section 3.

2. Modelling of unsteady thermal conduction by Brownian walkers

2.1 Numerical structure

Modelling unsteady conductive heat transfer is based on the random displacement of Brownian walkers within a numerical structure composed of a set of cubic elements having all the same volume and usually called “voxels” (three-dimensional extension of the pixel). With the purpose of limiting the memory impact on 3D simulations, no additional mesh refinement procedure is necessary. Then the edge of the voxel represents the smallest length scale of the microstructural description, and consequently this length corresponds to the spatial resolution of the heterogeneous medium. With a sufficiently fine resolution, this cubic discretization makes it possible to represent different types of structures (composite materials, foams with open or closed porosity, fibrous media) by precisely accounting for the microstructure. In addition, a voxel representation makes it possible to work directly on the reconstitutions provided by the experimental technique of X-ray tomography. Each voxel is characterised by two integer indices. The first one, n , characterizes the position of the voxel in the numerical structure. Knowledge of the position of the voxel is absolutely necessary in order to identify the treatment to which the voxel must be subjected during the simulation. In particular, if the voxel is located at a boundary of the calculation domain, it must be subjected to a boundary condition. A second index, m , characterizes the material constituting the voxel. Knowledge of the voxel constituent makes it possible to associate it with the thermophysical properties (thermal conductivity, density and specific heat) that will govern the transport of the walkers. Each voxel is therefore considered homogeneous and is made of a single material with isotropic thermophysical properties. The heterogeneous media used in the applications mentioned in the introduction are often made of two phases, a so-called fluid phase filled with a gas or a liquid, and a solid phase that is considered as the skeleton of the material. The latter can itself be composed of several constituents. The representation by voxels makes it possible to take account of all the phases of a heterogeneous medium including the fluid phase of a porous medium. The thermophysical properties of each phase are attributed to each voxel

filled with this phase so as to model therein the heat transfer by conduction. Finally, our model is developed with a 3D vision. However, in this article, simple geometries (essentially 1D Cartesian) will be treated in order to validate the theoretical concepts. The denomination of voxel will be conserved in the following, even if the calculations illustrating the concepts developed are done in 1D.

2.2 The reference elementary enthalpy

Historically, very few studies [19,22] treat the diffusion of Brownian walkers in heterogeneous materials with a quantitative observation of the information transported by the walkers (quantities of atoms for the transport of species, enthalpy for the transport of heat). Yet, a quantitative approach is indispensable to model the diffusion of enthalpy in transient regime, an external heat power source and to ensure the conservation of the energy between all the present constituents or phases (fluid and solid). Thus, in this work, each walker is seen as an enthalpy carrying particle, moving in the numerical environment and participating by its movement in the conductive heat flux. This heat diffusion via the walkers generates the change in the temperature field within the material in the transient regime.

Our approach supposes that all the walkers carry the same quantity of enthalpy, defined as the reference elementary enthalpy. This approach was initiated by preceding authors [19,20,23]. The reference elementary enthalpy δh_r is defined by the following expression:

$$\delta h_r = \rho_r C_{pr} V_v \frac{\Delta T_c}{M_r} \quad (1)$$

where:

- ρ_r and C_{pr} are the density and the specific heat of one of the constituents of the heterogeneous medium, taken as the reference constituent.
- V_v is the volume of one voxel.
- ΔT_c represents a temperature elevation characteristic of the considered thermal problem. This temperature elevation is defined with respect to a reference temperature T_r . The enthalpy of a voxel is zero at the temperature T_r ; in other words, a voxel at the temperature T_r does not contain any walker. This temperature is therefore a relative zero representing the temperature of the medium in the absence of Brownian walkers.
- M_r is the number of walkers that produce a temperature elevation equal to ΔT_c in a voxel made of the reference constituent.

As each voxel, of volume V_v , is considered as homogeneous, the properties ρ_m and C_{pm} of the material m constituting this voxel make it possible to determine its temperature elevation with respect to the reference temperature T_r from the number of walkers occupying it. The local

temperature $T_n(t)$ of the voxel n made of the constituent m at the instant t is expressed by the formula:

$$T_n(t) = T_r + \frac{M_n(t)\delta h_r}{\rho_m C_{pm} V_v} = T_r + \frac{\rho_r C_{pr}}{\rho_m C_{pm}} \frac{M_n(t)}{M_r} \Delta T_c \quad (2)$$

where $M_n(t)$ is the number of walkers in the voxel n at the instant t . This temperature is assumed to be uniform across the entire voxel and is associated with the centre of the latter during the calculation of a temperature field. The notion of temperature is therefore not defined on the frontiers of the voxels or at the contact surfaces of neighbouring voxels.

2.3 Principle of walker displacement

The displacement of the walkers in the structure follows the Itô-Taylor stochastic scheme [24,25]. The walkers are virtual particles with no mass, and they cannot collide with other walkers during their movement. According to the Itô-Taylor algorithm, the displacement of a walker between two neighbouring instants t and $(t + \delta t)$ is characterised by the following expression:

$$\overrightarrow{\delta X(t)} = \vec{b} [\overrightarrow{X(t)}] \delta t + \overline{\delta c} [\overrightarrow{X(t)}] \overrightarrow{B(t)} \quad (3)$$

where:

- $\overrightarrow{X(t)}$ represents the position vector of the walker at the instant t , and $\overrightarrow{\delta X(t)}$ the displacement that it will carry out between the instants t and $(t + \delta t)$.
- $\vec{b} [\overrightarrow{X(t)}]$ is a velocity vector that can account for a macroscopic movement of the material (convective term) or for a thermal conductivity gradient. In our studies, the medium considered is motionless and the thermophysical properties of each constituent are assumed to be known and uniform within the same voxel; $\vec{b} [\overrightarrow{X(t)}]$ is therefore zero.
- $\overline{\delta c} [\overrightarrow{X(t)}]$ is a matrix of characteristic diffusion lengths. The generic component c_{ij} of this matrix has the following expression:

$$c_{ij} = \sqrt{2a_{ij}\delta t} \quad (4)$$

where the a_{ij} are the components of the diffusivity tensor of the constituent considered. Yet, each voxel of the numerical structure is assumed to contain a single constituent, and all the constituents are assumed to be isotropic. The diffusivity tensor is therefore reduced to the identity matrix multiplied by the diffusivity of the constituent considered.

- Finally, $\overrightarrow{B(t)}$ is a dimensionless random vector that represents the Brownian movement. Its three components come from independent random drawings according to the reduced centred normal distribution. The retained notation $\overrightarrow{B(t)}$ highlighting an apparent dependence of the

vector \vec{B} on time t simply expresses that the vector \vec{B} must be updated (by new random drawings) at each new time step.

At the beginning of each time step, the Brownian walkers are uniformly distributed in the voxel they belong to. Each walker is thus given a position (one coordinate per space dimension) which will be the starting point of its displacement over the time step. By applying the scheme defined above in a three-dimensional Cartesian coordinate system, the final position of the walker (x_f, y_f, z_f) after the displacement, starting from the initial position (x_i, y_i, z_i) , is determined by the system of equations:

$$\begin{cases} x_f = x_i + \sqrt{2a_m \delta t} B_1(t) \\ y_f = y_i + \sqrt{2a_m \delta t} B_2(t) \\ z_f = z_i + \sqrt{2a_m \delta t} B_3(t) \end{cases} \quad (5)$$

During the displacement of a walker between two neighbouring instants, the trajectory of the latter is stored in memory so as to take account of the singularities that it could encounter (crossing the interface between two different constituents or reaching a boundary of the calculation domain). On the other hand, for computer resource reasons (quantity of 3D memory), the choice was made to not retain the exact position of the walker in the structure at the end of each step but only the number n of the arrival voxel. Hence, at the end of the displacement of a walker during a time step δt , its arrival voxel has its number of walkers simply increased by one unit and its departure voxel decreased by one unit. The flowchart of a typical Brownian walker calculation is illustrated in Figure 1. This procedure applied to each walker makes it possible to pass from the integer vector \vec{M}_t (number of walkers in each voxel n at the instant t) to its counterpart at the instant $(t + \delta t)$. For the treatment of the following time step, a new uniform distribution per voxel is applied so as to initialise the positions of the walkers for their future displacements.

For all the concepts demonstrated in the rest of Section 2, we shall work within a homogeneous medium. The treatment of heterogeneity will be addressed in Section 3.

2.4 Determination of the temporal resolution

The time step δt of the Brownian displacement (5) has to be adapted to the different input parameters of the simulation. To define the time step adapted to a given simulation, the following dimensionless ratio α is introduced:

$$\alpha = \frac{\sqrt{2a\delta t}}{\delta x} \quad (6)$$

This parameter appears as being the ratio of the characteristic diffusion length over the time duration δt to the spatial discretization δx . It indicates the order of magnitude of the number of

voxels that a walker crosses during one time step. The impact of the value of the time step δt (or of the parameter α) is studied by considering the following configuration:

- A 1D Cartesian medium of length L , homogeneous and of diffusivity a , is discretized in N voxels. This medium is initially at the reference temperature T_r .
- At the instant $t = 0$, the face $x = 0$, i.e. the voxel $n = 0$, is brought to the temperature $T_0 > T_r$. This temperature T_0 is maintained during the entire simulation by ensuring a constant number of walkers equal to the reference number M_r in the voxel $n = 0$. The face $x = L$, i.e. the voxel $n = N - 1$, is maintained at the temperature T_r , therefore with a number of walkers that is constantly zero. The procedure for maintaining a temperature in a voxel will be explained in Section 2.5. The characteristic temperature elevation of the problem is then defined by the expression $\Delta T_c = T_0 - T_r$.

The transient 1D conduction problem described above can be treated in a dimensionless form [26] by introducing the following quantities: $\Delta T^*(x^*, t^*) = \frac{T(x,t) - T_r}{\Delta T_c}$, $x^* = \frac{x}{L}$, $t^* = \frac{at}{L^2}$, $\delta X^*(t) = \frac{\delta X(t)}{L}$ and $\delta t^* = \frac{a\delta t}{L^2}$ (it can be demonstrated that δt^* and α are linked by the relationship $\alpha^2 = 2N^2\delta t^*$). $\Delta T^*(x^*, t^*)$ represents the dimensionless temperature elevation at the instant t^* in the voxel n whose centre is located at the abscissa x^* . In the modelling by Brownian walkers, the number of parameters governing the problem is then reduced to 3: N , M_r and δt^* . In all the calculations carried out in this article, the following values were attributed to the first two parameters: $(N, M_r) = (100, 2 \cdot 10^5)$. The reference number of walkers M_r was chosen in such a way that the stochastic noise generated by the random movement of the walkers is sufficiently low to not affect the precision and the relevance of the results. Several simulations on this experimental configuration with different time steps were then conducted. Although these problems could be treated in a dimensionless form, numerical values of the experiment parameters are listed here in order to help the physical representation and to compare with other models: $L = 10^{-2}$ m, $\Delta T_c = T_0 - T_r = 10$ K, $\lambda = 1$ W.m⁻¹.K⁻¹, $\rho C_p = 1 \cdot 10^5$ J.m⁻³.K⁻¹. Moreover, all validations of boundary conditions that will be presented in Section 2.5 have been simulated with the same numerical values and initial conditions.

In a first step, a simulation is carried out with a time step δt^* such that the ratio α equals 2. In this configuration, the walkers travel on average a few voxels per time step. Then, in order to attempt to improve the precision of the results of the transient regime, the choice is made to substantially decrease the time step by dividing δt^* by 100 (and therefore α by 10) (see Figure 2(a)). In a third simulation, the time step δt^* is now increased (δt^* is multiplied by 10, and therefore α passes to $2\sqrt{10} = 6.32$) so as to decrease the number of displacements to be calculated and to increase the distance travelled by the walkers at each time step. This method makes it

possible to reduce the calculation time of the simulation and to reach the asymptotic steady state more quickly (see Figure 2(b)). The results of these three simulations are then compared to those issued from a conventional finite differences calculation. This classical method of numerical resolution of partial differential equations simply consists of replacing the partial derivatives by approximations issued from Taylor expansions [27]. It is radically different from the walkers approach in that whereas the walkers approach is stochastic, the finite differences method is fundamentally deterministic. When dealing with transient diffusion problems, particular attention must be paid to the choice of the time step for a given space discretization. But a particular version of the finite differences method, based on a so-called implicit Euler scheme, makes the algorithm unconditionally stable, i.e. stable whatever the value retained for the time step of the calculation [27]. For all the finite differences calculation results that we show in this article, we have used the implicit Euler scheme.

In Figures 2(a) and 2(b), it is observed that the temperature profile obtained by Brownian walkers with $\alpha = 2$ coincides excellently with that obtained by finite differences. However the comparison of the black ($\alpha = 2$) and red ($\alpha = 0.2$) curves of Figure 2(a) shows that a decrease in the time step in the stochastic model has for consequence an artificial acceleration of the conductive transfer. This result is curious in light of the displacement procedure of the Brownian walkers. Indeed, the treatment of a time step begins with uniformly distributing the walkers in their respective departure voxels. The walkers are then displaced according to Equation (5), and only the numbers of the arrival voxels are retained at the end of the displacements. Thus, if the conductive time step is too low, few walkers change of voxel over one time step. Then they are randomly repositioned in the same voxel for the following time step. Intuitively, choosing a lower time step would therefore tend to slow down the heat transfer via the diffusion of the walkers. Yet, the exact opposite occurs. The explanation can be found in the choice of uniformly distributing the positions of the walkers at the initialisation of each time step. In the preceding transient 1D problem, the transfer results from an overall displacement of the walkers from “left” to “right”. At each time step, the walkers are uniformly distributed within the voxels. Thus a walker has as much chance to be located near the “left” face of its voxel as the “right” face. By decreasing the time step and therefore increasing the number of displacements of the walkers for the same final observation time, the walkers are distributed uniformly within the voxels more often. Consequently, the walkers have more occasions to be located near the right face of their voxel and to cross this face during their displacement. At the end of this displacement, they will be considered as belonging to the voxel on the right. Then they will be uniformly distributed in the latter by the same procedure at the initialisation of the following time step, thus resulting in this artificial acceleration. 1D simulations (not shown here) conducted by retaining the exact positions of the walkers at the end of each time

step have confirmed this interpretation. However, retaining the exact positions causes other problems that will not be detailed here and substantially increases the impact on the computer memory as well as the durations of the simulations, proportionately to the number of walkers and the space dimension. In the perspective of future 3D calculations, we have decided not to retain this modelling strategy.

Figure 2(b) shows that the increase in the time step ($\alpha = 6.32$) causes the appearance of two temperature jumps in the vicinity of the walls with imposed temperatures. An excessively long time step then has for consequence of biasing the spatial distribution of the walkers in the medium. Our calculations have shown that these jumps are also present during the transient regime. This is a serious weakness of the Brownian walkers approach: reaching the asymptotic steady state requires the correct and complete resolution of the transient regime and therefore the successive displacements of many walkers over sufficiently short time steps.

The results of Figure 2 highlight the importance of the choice of the parameter α for a correct resolution of the heat transfer by Brownian walkers. A bad choice of α causes an incorrect distribution of the walkers (in volume and at the boundaries) and therefore a temperature field that does not correspond to the physics of the heat transfer by conduction. The many tests that we have conducted have led us to the conclusion that the value of the time step for which $\alpha \approx 2$ represents a good compromise between precision of the results (α sufficiently small, but not too small in order to prevent the problems of artificial acceleration of the heat transfer) and rapidity of the calculation (α large enough, but not too large so as to prevent the temperature jump problems at the boundaries). This criterion will be applied for all the simulations of Section 2.5 dealing with a homogeneous medium. The choice of the time step will be more delicate in the presence of different constituents, characterized by different thermal diffusivities. This point will be addressed in Section 3.

2.5 Modelling various boundary conditions

The implementation of boundary conditions in the simulations, adapted to the voxelized representation of the structure and to the stochastic movements of the walkers, has to be stated. These boundary conditions (Dirichlet, Neumann, Newton) must be applied at each time step of the simulation in a scheme that is unsteady by nature due to the movements of the walkers. The ability to apply these conditions is absolutely necessary in the objective of modelling different thermal configurations, in particular conventional thermal characterization experiments such as the so-called “guarded hot plate” and “flash” techniques.

2.5.1 Dirichlet condition (imposed temperature)

In our approach, the temperature field is defined only at the centres of the voxels, not on their frontiers. The temperature of each voxel is calculated by taking account of the enthalpy present and the constituent of the voxel. In order to impose a temperature at a boundary, all the voxels in contact with this border are considered as walker reservoirs. The numbers of walkers in these reservoir voxels must be updated at each time step after the displacements of the walkers in order to ensure the Dirichlet condition. Due to the constant movements of all the walkers, a portion of the walkers present in a reservoir voxel at an instant t diffuses within the medium between this instant t and the following instant $(t + \delta t)$. Likewise, certain walkers coming from other voxels can populate the reservoir voxel during this time interval. Regulating the enthalpy of the reservoir voxel then consists simply of replacing the number of walkers in the voxel at the end of the time step with the correct value before the initialisation of the following time step. The number of walkers to maintain depends on the nature of the constituent of the voxel via its thermophysical properties (ρC_p). In addition, in order to impose a displacement of the walkers from the reservoir voxel to the medium and to prevent them from exiting the numerical structure, the external faces of the reservoir voxel are made adiabatic: a walker that encounters one of these faces is specularly reflected, and its remaining travel length is conserved.

In order to validate these concepts, the thermal problem introduced in Section 2.4 (1D Cartesian diffusion in a homogeneous medium subjected to two imposed temperatures) is treated again. The results in transient regime of the simulation by walkers with $\alpha = 2$ are presented and compared with those obtained by finite differences in Figure 3. Firstly, compliance with the Dirichlet boundary conditions during the entire simulation by walkers is observed: the temperatures elevations $\Delta T^* = 1$ and $\Delta T^* = 0$ are indeed maintained at the ends of the medium all along the transient regime to the asymptotic steady state. In addition, the temperature elevation profiles provided by the walkers coincide excellently with those obtained by finite differences at each instant considered. Therefore, the introduction of reservoir voxels where the number of walkers is regulated and whose outer borders are made adiabatic makes it possible to simulate Dirichlet type (imposed temperature) boundary conditions.

2.5.2 Neumann condition (imposed flux)

An imposed flux condition on a border represents an injection of enthalpy at an imposed rate in the medium and consequently the creation of walkers penetrating into the medium through this border. This injection consists of launching a number of walkers that corresponds exactly to the enthalpy from a unique position and in the correct direction. Thus, in a 1D Cartesian geometry (interval $[0 ; L]$) and for an imposed flux at the border $x = 0$, all the walkers accounting for this incident flux are initially located at the abscissa $x = 0 + \varepsilon$ where ε is a very small length with

respect to the step δx of the spatial discretization, i.e. very close to the border where the flux boundary condition is imposed. Moreover, the walkers must be injected in the direction of increasing x . To do this, the first idea consists of making the plane $x = 0$ adiabatic so that the walkers launched in the direction of decreasing x are specularly reflected at this plane. But it has been shown that proceeding so results in a lack of walkers in the vicinity of the wall [28]. We think that this default is due to the assumption of adiabatic wall: reflecting the walkers “to the right” at this wall produces overconcentrations of walkers far from the wall compared to the concentration at the wall, so that finally the temperature slope at the wall has an opposite sign to the temperature slope imposed by the flux. In addition, no walker can come from a negative initial position because the walkers that model the imposed flux are introduced in the medium from the unique position $x = 0 + \varepsilon$. Elements for the resolution of this problem can be found in [28]. Let us place, on the “left” side of the border $x = 0$, a semi-infinite medium ($x \leq 0$) filled with the same homogeneous material and supposed isothermal. In this situation, the number of walkers per unit volume C is uniform within the semi-infinite medium (this point will be more detailed in Section 2.5.3). Consequently, the number of walkers present in a segment $[x \leq 0 ; x + dx]$ of the semi-infinite medium of section S is $dM = CSdx$, and the number of these walkers that will be located in the segment $[l \geq 0 ; l + dl]$ after their displacements is:

$$dM \times \frac{1}{\eta\sqrt{2\pi}} \exp\left(-\frac{(l-x)^2}{2\eta^2}\right) dl = \frac{CSdx}{\eta\sqrt{2\pi}} \exp\left(-\frac{(l-x)^2}{2\eta^2}\right) dl \quad (7)$$

where $\eta = \sqrt{2a\delta t}$ is the standard deviation of the centred normal distribution in the standard Itô-Taylor algorithm (Equation (5)). Integrating Equation (7) over all the possible initial positions of the walkers (comprised between $-\infty$ and 0) provides the total number of walkers of the semi-infinite medium that are located in the segment $[l \geq 0 ; l + dl]$ after their displacements. This number $dM(l \geq 0)$ is equal to:

$$dM(l \geq 0) = \int_{-\infty}^0 \frac{CSdx}{\eta\sqrt{2\pi}} \exp\left(-\frac{(l-x)^2}{2\eta^2}\right) dl = \frac{CSdl}{2} \operatorname{erfc}\left(\frac{l}{\eta\sqrt{2}}\right) \quad (8)$$

This result shows that the probability density function associated with the random variable l has the following expression:

$$g(l \geq 0) \propto \frac{dM(l \geq 0)}{dl} = K \operatorname{erfc}\left(\frac{l}{\eta\sqrt{2}}\right) \quad (9)$$

where the symbol “ \propto ” means “proportional to” and K is a multiplicative constant which must be such that $\int_0^{+\infty} g(l)dl = 1$ (condition for normalizing the probability density function). This

condition yields $K = \frac{1}{\eta} \sqrt{\frac{\pi}{2}}$ and therefore:

$$g(l \geq 0) = \frac{1}{\eta} \sqrt{\frac{\pi}{2}} \operatorname{erfc}\left(\frac{l}{\eta\sqrt{2}}\right) = \sqrt{\frac{\pi}{4a\delta t}} \operatorname{erfc}\left(\frac{l}{\sqrt{4a\delta t}}\right) \quad (10)$$

It is thus demonstrated that taking into account the existence of walkers at negative x positions is equivalent to imposing the probability density function $g(l)$ expressed above to the injection lengths $l \geq 0$ of walkers created at the position $x = 0 + \varepsilon$. This is done practically by introducing the cumulative distribution function $G(l \geq 0)$ associated with the probability density function $g(l \geq 0)$:

$$G(l \geq 0) = \int_0^l g(x) dx = 1 - \sqrt{\pi} \operatorname{ierfc}\left(\frac{l}{\sqrt{4a\delta t}}\right) \quad (11)$$

Numerically resolving the equation $G(l) = r$, where r is a random number following the uniform distribution over $]0 ; 1[$, via the Newton-Raphson algorithm makes it possible to determine the travel lengths l of the walkers introduced to simulate the imposed flux. These lengths are evaluated based on the diffusivity of the constituent that occupies the departure voxel. Contrary to an imposed temperature boundary condition, the number of walkers injected during one time step at the boundary of a voxel subjected to an imposed flux boundary condition is independent of the nature of the voxel constituent.

To validate this strategy, the preceding transient 1D Cartesian thermal problem is considered again with the same parameters (N, M_r, α) ; at $x = 0$, the Dirichlet condition is simply replaced with a Neumann condition with a surface heat flux of intensity φ_0 that is constant over time. The number of walkers per surface unit M_S to have entered through the boundary $x = 0$ at each time step so as to give account of this heat flux is given by the formula:

$$M_S = \frac{\varphi_0 \delta t}{\delta h_r} \quad (12)$$

Figure 4 shows the dimensionless temperature elevation profiles $\Delta T^* = \frac{T-T_L}{\varphi_0 L/\lambda}$ versus the dimensionless abscissa $x^* = \frac{x}{L}$ at different dimensionless instants $t^* = \frac{at}{L^2}$ obtained by walkers on the one hand and by finite differences on the other hand. Here again, the correspondence between the walker simulations and the finite difference results is quite satisfactory. At the instant $t^* = 2$, the asymptotic steady state is reached and the temperature field follows a linear profile. The procedure for modelling a Neumann boundary condition (imposed heat flux) by the injection of walkers with an ad hoc probability law is therefore validated.

2.5.3 Newton condition (convective heat transfer at a wall)

A convective heat exchange between a fluid of temperature T_{fl} and a solid wall of temperature T_{so} is characterized by a boundary condition combining the temperatures and the heat

flux. In the framework of the formalism of Brownian walkers to represent the transfer of heat, this condition at the boundary must be treated stochastically: what is the future of a walker when it encounters a boundary subjected to a heat exchange by convection, and how to model this type of boundary condition? A stochastic criterion of reflection or transmission of the walkers at the boundary must be determined, the transmissions accounting for of the convective heat losses.

Let us consider a semi-infinite space ($x \leq 0$), filled with a solid homogeneous medium of diffusivity $a = \frac{\lambda}{\rho C_p}$, isothermal at the temperature T_{so} . The other semi-infinite space ($x \geq 0$) is filled with a homogeneous fluid at the uniform temperature T_{fl} . The reference temperature for the enthalpy calculations T_r is chosen equal to T_{fl} . The enthalpy H contained in a volume element ΔV of the solid medium is $H = \rho C_p \Delta V (T_{so} - T_{fl})$ where ρ and C_p refer to the solid material. In addition, if M is the number of walkers present in this volume element, we have $H = M \delta h_r$, and therefore:

$$\frac{M}{\Delta V} = \frac{\rho C_p (T_{so} - T_{fl})}{\delta h_r} = \text{constant } C \quad (13)$$

C represents the number of walkers per unit volume in the semi-infinite medium ($x \leq 0$). Now let us consider a walker of this semi-infinite medium initially at the position $x \leq 0$. Its displacement between the instant t and the instant $(t + \delta t)$ is calculated using Equation (5). During this time step, the walker crosses the boundary $x = 0$ of the semi-infinite medium if $x + \sqrt{2a\delta t} B_1 \geq 0$ i.e. if $B_1 \geq -\frac{x}{\sqrt{2a\delta t}}$. Thus, for a fixed initial position $x \leq 0$, the conditional probability \mathcal{P}_{tr} that the walker crosses the boundary $x = 0$ between t and $(t + \delta t)$ is $\mathcal{P}\left(B_1 \geq -\frac{x}{\sqrt{2a\delta t}}\right)$ where B_1 is a random number following the reduced centred normal distribution. The calculation of this probability gives:

$$\mathcal{P}_{tr} = \mathcal{P}\left(B_1 \geq -\frac{x}{\sqrt{2a\delta t}}\right) = \frac{1}{2} \operatorname{erfc}\left(-\frac{x}{2\sqrt{a\delta t}}\right) \quad (14)$$

The number of walkers present in a segment $[x; x + dx]$ of the solid medium of section S is $dM = CSdx$. Consequently, the number of walkers originating from this segment that will cross the boundary $x = 0$ during a time step has for expression:

$$dM \times \mathcal{P}_{tr} = \frac{CSdx}{2} \operatorname{erfc}\left(-\frac{x}{2\sqrt{a\delta t}}\right) \quad (15)$$

The integration of (15) over all the possible initial positions of the walkers (comprised between $-\infty$ and 0) provides the total number of walkers of the semi-infinite medium that cross the boundary between t and $(t + \delta t)$. This number M_{tr} is equal to:

$$M_{tr} = \int_{-\infty}^0 dM \times \mathcal{P}_{tr} = CS \sqrt{\frac{a\delta t}{\pi}} \quad (16)$$

The surface flux crossing the boundary during the time step δt due to the movements of the walkers is then:

$$\varphi = \frac{M_{tr}\delta h_r}{S\delta t} = C \sqrt{\frac{a\delta t}{\pi}} \frac{\delta h_r}{\delta t} = C\delta h_r \sqrt{\frac{a}{\pi\delta t}} = \rho C_p (T_{so} - T_{fl}) \sqrt{\frac{a}{\pi\delta t}} \quad (17)$$

In Equation (17), the thermal effusivity $e = \rho C_p \sqrt{a} = \sqrt{\lambda \rho C_p}$ of the solid medium appears. The thermal effusivity of a material characterizes the ability of the latter to impose its temperature and therefore generate a heat flux. Thus the surface flux generated by the walkers crossing the interface $x = 0$ in the direction solid \rightarrow fluid during the time interval δt has for expression:

$$\varphi_{so \rightarrow fl} = \frac{e(T_{so} - T_{fl})}{\sqrt{\pi\delta t}} \quad (18)$$

On the other hand, the surface flux crossing the interface $x = 0$ in the direction fluid \rightarrow solid, of convective nature, has for expression:

$$\varphi_{fl \rightarrow so} = h(T_{fl} - T_{so}) \quad (19)$$

where h stands for the convective heat transfer coefficient at the interface. We therefore have:

$$\left| \frac{\varphi_{so \rightarrow fl}}{\varphi_{fl \rightarrow so}} \right| = \frac{e}{h\sqrt{\pi\delta t}} \quad (20)$$

When the solid and the fluid are in a situation of perfect thermal equilibrium ($T_{so} = T_{fl}$), these two flux must be equal. Yet, imagine that the quantity $\frac{e}{h\sqrt{\pi\delta t}}$ on the right hand side of Equation (20) is greater than 1. Then $|\varphi_{so \rightarrow fl}| > |\varphi_{fl \rightarrow so}|$, in other words the heat flux passing from the solid to the fluid is excessive. It is therefore necessary to attenuate the flux $|\varphi_{so \rightarrow fl}|$, or equivalently the number of walkers, passing from the solid to the fluid by multiplying it by $\frac{h\sqrt{\pi\delta t}}{e} < 1$. To carry out this operation in the model, the following stochastic procedure is applied:

- For each walker impacting the interface, a random number r is drawn following the uniform distribution on $]0 ; 1[$ and compared to $\frac{h\sqrt{\pi\delta t}}{e}$;
- If $\leq \frac{h\sqrt{\pi\delta t}}{e}$, the walker is transmitted to the surrounding fluid. Thus it “disappears” and represents a convective enthalpy loss for the solid medium;
- Otherwise, it is specularly reflected in the medium.

Thus the transmission criterion of a walker encountering a boundary subjected to convective heat losses is expressed by the test:

$$r \leq \mathcal{P}_{conv} = \frac{h\sqrt{\pi\delta t}}{e} \quad (21)$$

This criterion depends solely on the effusivity of the material and therefore remains constant throughout the entire simulation. Its validity is tested by again considering a homogeneous 1D Cartesian medium $[0; L]$ initially at the uniform temperature T_r . The simulation conditions are unchanged $((N, M_r, \alpha) = (100, 2 \cdot 10^5, 2))$. At the instant $t = 0$, the border $x = 0$ of the medium is brought to and maintained at a temperature $T_0 > T_r$, while its border $x = L$ is subjected to a convective heat exchange of coefficient h with a surrounding fluid of characteristic temperature equal to T_r . The conductivity λ and the product ρC_p of the medium are respectively equal to $1 \text{ W.m}^{-1}.\text{K}^{-1}$ and $1 \cdot 10^5 \text{ J.m}^{-3}.\text{K}^{-1}$, so that its effusivity e is approximately $316 \text{ J.K}^{-1}.\text{m}^{-2}.\text{s}^{-1/2}$. The width of the domain L is taken equal to 1 cm. Three values of the Biot number $Bi = \frac{hL}{\lambda}$ corresponding to different values of the heat transfer coefficient h are examined in order to study the validity of the criterion (21) in extreme situations: (a) $Bi = 0$ yielding $\mathcal{P}_{conv} = 0$, (b) $Bi = 0.5$ yielding $\mathcal{P}_{conv} = 0.013$, and (c) $Bi = 100$ yielding $\mathcal{P}_{conv} = 2.5$ (the values of \mathcal{P}_{conv} are calculated with $\delta t = 2 \cdot 10^{-3} \text{ s}$, value corresponding to $\alpha = 2$). Figures 5(a), 5(b) and 5(c) show the dimensionless temperature elevation profiles $\Delta T^* = \frac{T - T_r}{T_0 - T_r}$ versus the dimensionless abscissa $x^* = \frac{x}{L}$ at different dimensionless instants $t^* = \frac{at}{L^2}$ obtained by walkers on the one hand and by finite differences on the other hand for the three values of Bi mentioned above.

On each one of the three figures, the temperature elevation profiles are plotted at instants that cover the transient regime to the asymptotic steady state. The procedure presented above for managing walkers encountering a border subjected to convective heat losses makes it possible to give an account of the change in the temperature within the medium at each instant. According to this procedure and the expression of \mathcal{P}_{conv} , imposing a convective loss condition with a zero exchange coefficient h , i.e. imposing a condition of adiabaticity, is equivalent to imposing a zero value to \mathcal{P}_{conv} . Criterion (21) is therefore never satisfied, and any walker encountering the interface is specularly reflected within the medium. This results, in Figure 5(a), in temperature profiles that all have a horizontal tangent in $x^* = 1$ at each instant of the transient state and in a homogenization at the temperature elevation $\Delta T^* = 1$ in all the medium when the asymptotic steady state is reached. This temperature space-time field is indeed the expected result in light of the conditions of the problem treated (adiabatic boundary condition at $x^* = 1$). On the contrary, imposing a convective exchange with a fluid characterized by a very large value of the transfer coefficient is equivalent to imposing the characteristic temperature of the fluid at the interface. With a Biot number $Bi = 100$, the parameter \mathcal{P}_{conv} equals $2.5 > 1$. Thus any walker encountering the face $x = L$ of the structure is

transmitted to the ambient fluid, which is equivalent to considering that the fluid imposes its temperature at the contact with the sample like a thermostat. Figure 5(c) illustrates this phenomenon since the temperature profiles exhibited on this graph are consistent with those of Section 2.5.1 devoted to the modelling of boundary conditions of imposed temperatures. The stochastic transmission criterion (21) to give account of convective heat losses by means of Brownian walkers is therefore validated, even for extreme values of the exchange coefficient.

2.5.4 Flash pulse excitation

The study of the thermal behaviour of materials is based in part on experimental characterization techniques that make it possible to estimate the thermophysical properties of the latter at the macroscopic scale. The so-called “flash method” experimental technique [29] is one of the most widespread characterization methods of thermal properties. It makes it possible to estimate the thermal diffusivity of the material without contact and up to high temperatures. The flash method consists of imposing a uniformly distributed pulse flux at the front face of the sample to be characterized, and measuring the curve of the change over time of the temperature of the front face of the sample [30,31] or of its rear face [13,32]. The technique has been improved over the years to be applied on semi-transparent materials [33, 34] like polymer foams [35] for example. In this article, we focus on the flash method called “rear face flash method”, and we consider that conduction is the only transfer mode within the sample.

Our objective is to manage to reproduce a rear face flash thermogram, by means of Brownian walkers, that can be used like an experimental thermogram to estimate the phonic thermal diffusivity of the material by adapted inverse methods. This objective requires being in a position to model the different key points of the flash method with our stochastic process. In pure conduction, the change in the temperature at the rear face is governed by the thermal excitation of the medium (intensity and duration of the irradiation), the thermal diffusion in the medium and the convective losses with the ambient fluid. The treatment of a uniform surface flux and of convective losses by Brownian walkers was examined above (see Sections 2.5.2 and 2.5.3). However, in the case of a flash experiment, the excitation pulse on the front face is of short duration. Because of this, the duration of application of the boundary condition now depends on the pulse duration of the source, noted t_{pulse} (from a few tens of microseconds to a few milliseconds). This duration t_{pulse} must be weighed against the time step of the simulations by walkers δt , the value of which, for a homogeneous medium, is imposed by the criterion $\alpha \approx 2$. Two cases are then to be distinguished:

- If $t_{pulse} < \delta t$, the thermal excitation pulse is considered as instantaneous (Dirac pulse). All the enthalpy, i.e. the corresponding number of walkers, is injected at the very first conductive time step.

- If $t_{pulse} > \delta t$, the enthalpy is distributed over all the time steps that constitute the pulse duration of the source. This procedure makes it possible to take account of the convolution between the temporal distribution of the excitation and the transient conductive heat transfer that is established within the medium. Moreover, the procedure described in the preceding section makes it possible to take account of the convective losses on the front and rear faces of the sample during the entire duration of the simulation, including the excitation phase.

For the purpose of validation, a 1D homogeneous medium of length $L = 2 \cdot 10^{-3}$ m and subjected to a heat pulse of intensity $\varphi_0 = 4 \cdot 10^4$ W.m⁻² on its front face is considered. The two boundaries of the medium are subjected to convective losses of exchange coefficient $h = 50$ W.m⁻².K⁻¹. The temporal parameters are equal to $\delta t = 8 \cdot 10^{-5}$ s and $t_{pulse} = 5 \cdot 10^{-3}$ s. The walkers are therefore uniformly injected during the first 63 time steps of the simulation corresponding to the interval $[0; t_{pulse}]$. The other simulation conditions are unchanged $((\lambda, \rho C_p, N, M_r, \alpha) = (1 \text{ W.m}^{-1}.\text{K}^{-1}, 1 \cdot 10^5 \text{ J.m}^{-3}.\text{K}^{-1}, 100, 2 \cdot 10^5, 2))$. The thermogram obtained is compared to the one issued from a finite differences calculation in the same simulation conditions (input parameters, temporal resolution) in Figure 6. The curves are made dimensionless by posing $\Delta T^* = \frac{T-T_r}{\Delta T_c}$ with $\Delta T_c = \frac{\varphi_0 t_{pulse}}{\rho C_p L} - T_r$. This quantity ΔT_c corresponds to the asymptotic temperature elevation reached at all points of the sample in the absence of convective losses. The two thermograms obtained correspond practically perfectly at each instant of the transient regime. The noise visible on the thermogram obtained by walkers (black curve) is the direct consequence of the stochastic nature of the approach. This thermogram has all the characteristics of a rear face thermogram resulting from a flash type excitation and where the thermal conduction is the only heat transfer mode considered: the slope of the thermogram at $t = 0$ is zero, and the temperature at the rear face increases to a maximum before decreasing due to the convective losses with the ambient medium. The very good correspondence of the two thermograms in the decreasing phase is an additional proof of the validity of the stochastic criterion (21) established to give account of the convective losses with Brownian walkers (see Section 2.5.3).

3. Taking account of the heterogeneity in a walker calculation

All of the concepts that make it possible to model the thermal diffusion and different boundary conditions (imposed temperature or flux, convective losses, pulse excitation) by means of Brownian walkers have been validated in the case of a homogeneous medium. However, the targeted media of study are heterogeneous (and in particular porous). This heterogeneity results in the presence of several constituents and consequently of interfaces within the voxelized

representation of the media. These internal interfaces can be of a solid-solid nature (for example in an insulating matrix charged with conductive particles), or of a fluid-solid nature when a porous medium is involved. Then, several questions appear concerning the behaviour of a walker when it encounters such an interface: does it have to be transmitted or reflected? Does the distance that remains to be travelled, which is retained when a walker is reflected in a specular manner at an adiabatic wall, have to be modified when the walker is transmitted and therefore continue its travel in a new constituent? Finally, the non-uniformity of the thermophysical properties results in that the criterion $\alpha = 2$ mentioned above for the choice of the time step δt cannot be verified simultaneously in all the constituents of the medium. So, how can the optimal time step be chosen? In this section, we attempt to answer these different questions.

3.1 Behaviour of a walker encountering the interface of two constituents

To demonstrate the procedure that applies in this situation, two 1D semi-infinite media are considered in contact at the level of the plane $x = 0$:

- The semi-infinite medium ($x \leq 0$) is filled with the constituent 1 characterized by the thermophysical properties $\rho_1 C_{p1}$, λ_1 and the effusivity $e_1 = \sqrt{\lambda_1 \rho_1 C_{p1}}$,
- Likewise, the semi-infinite medium ($x \geq 0$) is filled with the constituent 2 characterized by the thermophysical properties $\rho_2 C_{p2}$, λ_2 and e_2 .

It is moreover assumed that the two semi-infinite media are isothermal at the same temperature T_0 . Formula (18), demonstrated in Section 2.5.3, can be used here to express the surface heat flux produced by the walkers located initially in the medium 1 and crossing the interface $x = 0$ to the medium 2 during the time step δt : $\varphi_{1 \rightarrow 2} = \frac{e_1(T_0 - T_r)}{\sqrt{\pi \delta t}}$ where T_r is the reference temperature for the enthalpy. Likewise, the surface heat flux produced by the walkers located initially in the medium 2 and crossing the interface $x = 0$ to the medium 1 during the time step δt has for expression $\varphi_{2 \rightarrow 1} = \frac{e_2(T_0 - T_r)}{\sqrt{\pi \delta t}}$. This results in the equality:

$$\frac{\varphi_{1 \rightarrow 2}}{\varphi_{2 \rightarrow 1}} = \frac{e_1}{e_2} \quad (22)$$

The situation treated here is a perfect thermal equilibrium situation (because the two semi-infinite media are assumed to be isothermal at the same temperature); consequently, the ratio $\frac{\varphi_{1 \rightarrow 2}}{\varphi_{2 \rightarrow 1}}$ must be equal to 1. However, if we are in a situation where $e_1 > e_2$, then the flux $\varphi_{1 \rightarrow 2}$ is overestimated with respect to the flux $\varphi_{2 \rightarrow 1}$ and must therefore be attenuated in a ratio $\frac{e_2}{e_1}$. In other words, the fraction of the flux $\varphi_{1 \rightarrow 2}$ to be transmitted is equal to $\frac{e_2}{e_1}$. The correct transmission of the conductive flux at the interface of two voxels of different constituents is therefore carried out by

applying the following procedure. Consider a walker originating from the constituent 1 and that encounters an interface with the constituent 2. The transmission criterion of the walker through this interface is announced by:

$$r \leq \mathcal{P}_{tr} = \frac{e_2}{e_1} \quad (23)$$

where r is a random number drawn in the uniform distribution over $[0, 1]$. Note that if $e_2 < e_1$, only a fraction of the walkers is transmitted through the interface, while in the inverse case the walkers are transmitted without condition. Also note that if the two constituents have the same effusivity, the interface plays no role in the displacement of the walkers, which is consistent.

In the case of a transmission, it is necessary to take account of the change in the constituent over the remaining length to be travelled by the walker. In 2D, with the notations of Figure 7, the position M_{f1} of the walker is the result of the displacement calculated using Equation (5) by considering the diffusivity of the starting material (material 1) of the walker. If the diffusivity of the arrival material (material 2) is different, it must be taken into account in the determination of the correct final position of the walker. The travel lengths being related to the characteristic thermal diffusion length $\sqrt{2a\delta t}$ in the Itô-Taylor scheme, one may anticipate that the new final position M_{f2} is obtained by multiplying the distance that remains to be travelled in the new medium by the square root of the ratio of the diffusivities:

$$\overrightarrow{BM_{f2}} = \sqrt{\frac{a_2}{a_1}} \overrightarrow{BM_{f1}} \quad \text{consequently} \quad \left\{ \begin{array}{l} x_{f2} = x_B + \sqrt{\frac{a_2}{a_1}} (x_{f1} - x_B) \\ y_{f2} = y_B + \sqrt{\frac{a_2}{a_1}} (y_{f1} - y_B) \end{array} \right\} \quad (24)$$

In order to validate the procedure described above, a bilayer 1D Cartesian medium $[0 ; L]$ is considered. The first layer is constituted of a material 1 and is located at the abscissas $\in [0 ; \frac{L}{2}]$, and the second layer is constituted of a material 2 and is located at the abscissas $x \in [\frac{L}{2} ; L]$. In each one of the simulations, the whole medium is initially at the temperature T_r . At the instant $t = 0$, the faces $x = 0$ and $x = L$ are maintained respectively at $T_0 > T_r$ and T_r . In a first step, the thermophysical properties of the two constituents are chosen such that $a_1 = a_2$ but $e_1 \neq e_2$. This first choice of parameters makes it possible to test the transmission criterion at the level of the interface, which only involves the effusivities. In addition, it makes it possible to define a time step for which the criterion $\alpha = 2$ is verified for the two constituents. As $a_1 = a_2$, the distance that remains to be travelled by walker after a transmission is not affected by the change in constituent. Two effusivity contrasts were considered: $\frac{e_2}{e_1} = 2$ and $\frac{e_2}{e_1} = 10$. For $\frac{e_2}{e_1} = 2$, the thermophysical

properties are set to: $\lambda_1 = 1 \text{ W.m}^{-1}.\text{K}^{-1}$, $\lambda_2 = 4 \text{ W.m}^{-1}.\text{K}^{-1}$, $\rho_1 C_{p1} = 1 \cdot 10^5 \text{ J.m}^{-3}.\text{K}^{-1}$ and $\rho_2 C_{p2} = 4 \cdot 10^5 \text{ J.m}^{-3}.\text{K}^{-1}$. For $\frac{e_2}{e_1} = 10$, the thermophysical properties are set to: $\lambda_1 = 1 \text{ W.m}^{-1}.\text{K}^{-1}$, $\lambda_2 = 10 \text{ W.m}^{-1}.\text{K}^{-1}$, $\rho_1 C_{p1} = 1 \cdot 10^5 \text{ J.m}^{-3}.\text{K}^{-1}$ and $\rho_2 C_{p2} = 1 \cdot 10^6 \text{ J.m}^{-3}.\text{K}^{-1}$. The results are presented in Figures 8(a) and 8(b).

These figures show a very good correspondence between the temperature profiles obtained by finite differences and the simulations by Brownian walkers, with different effusivity contrasts, in particular in the vicinity close to the interface. This correspondence is true in the transient regime as well as in the asymptotic steady state. As the two constituents have the same diffusivity, the characteristic diffusion time through the sample $t_c = \frac{L^2}{a}$ is equal to 10 s; and it is observed in the two figures that at the instant $t = 20 \text{ s}$ the asymptotic steady state is reached (profiles $T(x)$ linear by pieces), which is consistent. Hence, these simulations demonstrate the validity of the criterion based on the effusivities (23) for the management of the walkers during the encounter with an internal interface.

3.2 Problem of the choice of the time step in the presence of a diffusivity contrast

Now, the two constituents considered in the bilayer medium no longer have the same diffusivity. So, the procedure described in the preceding section of adapting the distance remaining to be travelled by a transmitted walker has to be validated. In addition, the choice of the time step is complicated due to the impossibility of respecting the criterion $\alpha = 2$ for the two constituents. The problem is therefore the following: which constituent has to govern the choice of the time step? To answer this question, four analogous simulations are carried out, always in the case of 1D diffusion and with imposed temperature boundaries, but each one representing a different configuration. In all of the simulations, a bilayer medium is considered of which the two layers are of the same thickness. The two constituents (material 1 and material 2) have the same thermal inertia ($\rho_1 C_{p1} = \rho_2 C_{p2} = 1 \cdot 10^5 \text{ J.m}^{-3}.\text{K}^{-1}$), and their conductivities are respectively $\lambda_1 = 1 \text{ W.m}^{-1}.\text{K}^{-1}$ and $\lambda_2 = 4 \text{ W.m}^{-1}.\text{K}^{-1}$. We are therefore in the presence of a binary medium that has an effusivity contrast $\frac{e_2}{e_1} = 2$ and a diffusivity contrast $\frac{a_2}{a_1} = 4$. The different configurations examined differ:

- By the position of the constituents in the bilayer: the material 2 occupies the “left” layer ($0 \leq x^* \leq 0.5$) and the material 1 occupies the “right” layer ($0.5 \leq x^* \leq 1$) for cases (a) and (b), and the positions of the two materials are inverted for cases (c) and (d).
- By the constituent chosen for setting the time step: material 1 for cases (a) and (d), and material 2 for cases (b) and (c). The values of the parameters α_i corresponding to the two

constituents are therefore the following: $(\alpha_1, \alpha_2) = (2, 4)$ for cases (a) and (d), and $(\alpha_1, \alpha_2) = (1, 2)$ for cases (b) and (c).

The results of the four simulations are disclosed in Figure 9.

In Figure 9(a), the overall evolution of temperature in the medium follows the same trend for the two numerical simulations. However, a systematic delay in the temperature profile issued from the walkers with respect to that obtained by finite differences is observed. This delay is due to the influence of the time step at the level of the application of the imposed temperature boundary conditions. In this configuration, the choice of the time step was set by taking as a reference the material 1 placed over the interval $0.5 \leq x^* \leq 1$. This leads to a parameter $\alpha_2 = 4$ over the interval $0 \leq x^* \leq 0.5$, which generates a temperature jump at $x^* = 0$ (see Section 2.4). In the following simulation (Figure 9(b)), the bilayer is unchanged, but the time step is here set according to the most diffusive medium ($\alpha_1 = 1$ and $\alpha_2 = 2$). A very slight difference in the temperature in the vicinity of the interface between the two layers, which we cannot explain, is here observed when the asymptotic steady state is reached. For the rest, the temperature profile obtained by Brownian walkers has excellent coherence with the finite differences results. Based on these first two graphs, it therefore seems preferable to base the choice of the time step on the most diffusive constituent in order to have parameters α_i lower or equal to 2.

But it is also interesting to examine the impact of the constituent through which the walkers enter into the medium. In the configuration that we are studying, the thermal load is applied to the face $x = 0$, and therefore this face is the point of entry of the walkers. In the two preceding simulations, the walkers were entering through the most diffusive constituent (material 2). Here, as the two constituents are interchanged (Figures 9(c) and 9(d)), the walkers are entering through the least diffusive constituent. Figure 9(c) shows that by setting the time step in such a way that $\alpha_2 = 2$ (and therefore $\alpha_1 = 1$), therefore by referring to the most diffusive medium located over the interval $0.5 \leq x^* \leq 1$, the walkers artificially accelerate the heat transfer, in particular within the constituent 1 corresponding to $0 \leq x^* \leq 0.5$. This result is consistent with those observed in Section 2.4. In Figure 9(d), the time step was set in such a way that $\alpha_1 = 2$ (and therefore $\alpha_2 = 4$), therefore by taking as a reference the least diffusive medium located over the interval $0 \leq x^* \leq 0.5$. A difference between our model by Brownian walkers and the finite differences results, in particular in the steady state, can be observed in the most diffusive constituent. Indeed, the simulation conditions of Figure 9(d) have the consequence of creating a temperature jump in the vicinity of the thermostat at $x^* = 1$. However, in this voxel the temperature elevation $\Delta T^* = 0$ is regulated by ensuring therein the absence of walkers at each instant. The effect of the temperature jump is therefore lessened with respect to that observed in Figure 9(a).

In light of the results presented in the last four figures, it seems to us that the most satisfactory solution is to set the time step with reference to the medium in contact with the hot wall (see Figure 9(b)). We will use this criterion as a basis for the following studies of the article. Moreover, the very good general agreement observed in Figure 9 between the walker results and those obtained by finite differences validates the procedure of adapting the remaining lengths to be travelled by the transmitted walkers described in Section 3.1 (Equation (24)).

3.3 Analysis of a situation with a high contrast in thermophysical properties

In the preceding section, the procedure treating the heterogeneity was validated in the case of a moderate contrast in properties. In order to limit the undesirable effects related to the non-uniqueness of the value of the diffusivity in the medium, it was established that the best solution consists of taking the constituent in contact with the hot wall as the reference for determining the time step (via the relationship $\alpha = 2$). This procedure is now implemented to model the thermal diffusion within a 1D Cartesian medium of length $L = 1$ cm, composed of an alternation of layers of air and zirconia. This spatial configuration can be considered as being a very simplified representation of a felt constituted of zirconia fibres plunged in the air. These heterogeneous materials, used as thermal superinsulators at high temperatures, have strong contrasts in thermophysical properties of their constituents, since the diffusivity of the zirconia is $a_{ZrO_2} \approx 3.8 \cdot 10^{-7} \text{ m}^2 \cdot \text{s}^{-1}$ while that of the ambient air is $a_{air} \approx 2.3 \cdot 10^{-5} \text{ m}^2 \cdot \text{s}^{-1}$. Likewise, the effusivities of these two media are $e_{ZrO_2} \approx 1600 \text{ J} \cdot \text{K}^{-1} \cdot \text{m}^{-2} \cdot \text{s}^{-1/2}$ and $e_{air} \approx 5.3 \text{ J} \cdot \text{K}^{-1} \cdot \text{m}^{-2} \cdot \text{s}^{-1/2}$. The ratios of effusivity and of diffusivity are therefore respectively $\frac{e_{ZrO_2}}{e_{air}} \approx 300$ and $\frac{a_{ZrO_2}}{a_{air}} \approx \frac{1}{61}$. What impacts do these strong contrasts have on the results of our calculations by Brownian walkers? Is the strategy established in the preceding section consisting of choosing the material in contact with the hot wall as the reference for the choice of the time step still valid?

The material configuration retained is the following: the layers of zirconia are located over the ranges $0 \leq x^* \leq 0.1$, $0.2 \leq x^* \leq 0.45$, $0.55 \leq x^* \leq 0.7$ and $0.8 \leq x^* \leq 1$, and air occupies the remaining ranges. Initially, the medium is isothermal at the temperature T_r . At $t = 0$, the face $x = 0$ of the medium is subjected to the imposed temperature $T_0 > T_r$ while the face $x = L$ is maintained at the temperature T_r . As the constituent in contact with the hot wall is zirconia, in accordance with the conclusions of Section 3.2, the time step is chosen such that $\alpha_{ZrO_2} = 2$, which results in $\alpha_{air} = \alpha_{ZrO_2} \sqrt{\frac{a_{air}}{a_{ZrO_2}}} \approx 14$. In the case of a zirconia \rightarrow air transmission, the diffusivity contrast results in a multiplication by $\sqrt{61} \approx 8$ of the distance remaining to be travelled by the walker. It is then likely that during its new travel the walker will encounter new interfaces. During each time step, the calculation must then account for the multiple interfaces over the complete

travels of the walkers, until they arrive in their final voxels. Figure 10 presents the temperature profiles obtained by Brownian walkers at different instants of the transient state. Due to the very low diffusivity of zirconia, these instants correspond to the very beginning of the heat transfer within the multilayer sample. Thus an enlargement of the profiles over a portion of the calculation domain ($0 \leq x^* \leq 0.3$) is represented in this figure. Temperature jumps, without any physical justification, are observed at the interfaces. They are due to the high contrast in diffusivity between the two constituents that results in a large difference between the average lengths of travel in zirconia and in air. The strategy consisting of referring to the material in contact with the hot wall to set the time step appears therefore ineffective in the presence of large contrasts in properties.

It is however possible to access the asymptotic steady state of the thermal problem via the following subterfuge. In this state, only the thermal conductivities play a role in the heat transfer and the volume specific heats ρC_p of the different constituents have no influence. Thus, if the objective sought is limited to determining the asymptotic steady state, we are totally free to choose the values of the products ρC_p of the two constituents, and in particular it is possible to adapt one of these two values in such a way that the two diffusivities a_{air} and a_{ZrO_2} become equal. This trick then makes it possible to choose the time step in such a way that the criterion $\alpha = 2$ is verified for the two constituents. In these conditions, the crossing of an interface by a walker does not result in a modification of its displacement length. Of course, the transient state is biased by the modification of one of the two products ρC_p ; but if only the asymptotic steady state is sought, this strategy a priori seems acceptable. In order to test it, the value of the product ρC_p of air was modified in order to equalize the diffusivities of the two constituents. Then the calculation by walkers was launched until the asymptotic steady state was accessed. Figure 11 compares the result of this calculation with the exact stationary solution. The temperature profile in the asymptotic steady state obtained by Brownian walkers now corresponds very well to the exact stationary solution. It is thus demonstrated that the strategy consisting of modifying the volume specific heats ρC_p of the constituents with the purpose of equalising their diffusivities allows the proper calculation by Brownian walkers of the steady state temperature field within a heterogeneous medium that has substantial contrasts between the thermal properties of its constituents. This strategy can therefore be retained when the calculations concern only seeking the steady state.

The steady state thermal study of a heterogeneous medium is often carried out with the purpose of estimating its effective conductivity. The so-called “guarded hot plate” experimental technique is based on this principle: it consists of imposing a temperature difference between two faces of a sample of which all the other boundaries are perfectly insulated. Once the steady state is reached, the measurement of the thermal flux crossing the sample makes it possible to retrieve its effective conductivity. At the end of the simulation of this experiment with Brownian walkers, i.e.

when the steady state temperature profile is obtained, the Fourier law is applied between two neighbouring voxels in order to obtain the local conductive flux, then this flux is averaged over all the pairs of neighbouring voxels. The effective conductivity is then estimated and compared with the theoretical value issued from the model of thermal resistances in series. The calculations give respectively $\lambda_{eff}^{walkers} = 7.37 \cdot 10^{-2} \text{ W.m}^{-1}.\text{K}^{-1}$ and $\lambda_{eff}^{theory} = 7.27 \cdot 10^{-2} \text{ W.m}^{-1}.\text{K}^{-1}$. The excellent agreement between these two values once again validates our procedure of accessing the asymptotic steady state.

In conclusion, the procedures that we have described in Section 3.1 to take account of the heterogeneity in a calculation with walkers (criterion (23) for transmitting a walker on the one hand, and adapting the length of the remaining travel (Equation (24)) on the other hand) were certainly validated, but they are delicate to implement in the presence of constituents with highly contrasted thermal properties. On the other hand, if the objective of the calculation by walkers is limited to accessing the asymptotic steady state, then it is acceptable to modify the products ρC_p in such a way that all the diffusivities become equal. Then, the criterion $\alpha = 2$ can be verified for all the constituents of the medium. This strategy has the inconvenience of completely distorting the transient state. On the other hand, it is entirely pertinent for estimating the effective conductivity via the simulation of an experiment of the “guarded hot plate” type since interest is then given only to the asymptotic steady state.

4. Conclusion and perspectives

In this article, we have taken interest in adapting the stochastic simulation method by Brownian walkers to modelling the transient thermal conduction within heterogeneous media represented by voxelized structures. More precisely, we have determined the procedures that make it possible to choose the time step of the simulation, to give account of the conventional boundary conditions (imposed temperature, imposed surface flux, convective heat exchange), and to determine the behaviour of a walker encountering the interface of two constituents within the medium. We have shown that, in a homogeneous medium, the time step of the calculation δt should be chosen according to the spatial discretization step δx and the diffusivity of the medium a in such a way that the criterion $\alpha = \frac{\sqrt{2a\delta t}}{\delta x} = 2$ is respected. Concerning the imposed surface flux boundary condition, we have demonstrated and numerically validated the expression of the walker injection length distribution function that should be retained. Finally, we have demonstrated and numerically validated stochastic transmission criteria giving account of a convective heat transfer boundary condition in a walker calculation on the one hand and of the behaviour of a walker meeting the interface of two constituents on the other hand.

The next paths for work consist of carrying out numerical experiments for thermal characterization by means of our stochastic model on voxelized 2D or 3D structures representing REV of heterogeneous media. These 2D/3D structures will either be numerically generated academic geometries, or come from X-ray tomographies of real materials. In parallel, various paths are being studied in order to resolve the problems that have appeared in cases of high contrast in diffusivity at the level of the interfaces. An exact monitoring of the walkers, i.e. by retaining their exact positions at each time step, could resolve this problem, but the cost in terms of computer memory might be high. Finally, modelling the conduction-radiation coupling within porous media of complex architectures constitutes the final objective of our work. To do this, we are considering to resolve the radiative transfer by a stochastic method of ray tracing, to resolve the transient energy balance via our walker approach, and to couple the conductive and radiative modes via the space-time radiative power density field. This procedure will have to be applied during the entire transient regime, i.e. by calculating and by iterating until convergence of the temperature and radiative power density fields at each time step.

References

- [1] A. Kribus, Y. Gray, M. Grijnevich, G. Mittelman, S. Mey-Cloutier, C. Caliot, The promise and challenge of solar volumetric absorbers, *Solar Energy* 110 (2014) 463-481.
- [2] A. Ortona et al, SiSiC heat exchangers for recuperative gas burners with highly structured surface elements, *International Journal of Applied Ceramic Technology* 11 (2014) 927-937.
- [3] L. Ferrari et al, Sandwich structured ceramic matrix composites with periodic cellular ceramic cores: an active cooled thermal protection for space vehicles, *Composite Structures* 154 (2016) 61-68.
- [4] D. Rochais, G. Domingues, F. Enguehard, Numerical simulation of thermal conduction and diffusion through nanoporous superinsulating materials, 17th European Conference on Thermophysical Properties, Bratislava, Slovakia (2005), <https://hal.archives-ouvertes.fr/hal-01287483>.
- [5] T. Fiedler, I.V. Belova, G.E. Murch, Theoretical and Lattice Monte Carlo analyses on thermal conduction in cellular metals, *Computational Materials Science* 50 (2010) 503-509.
- [6] G.L. Vignoles, A. Ortona, Numerical study of effective heat conductivities of foams by coupled conduction and radiation, *International Journal of Heat and Mass Transfer* 109 (2016) 270-278.
- [7] R. Coquard, D. Baillis, Radiative characteristics of opaque spherical particle beds : a new method of prediction, *Journal of Thermophysics and Heat Transfer* 18 (2004) 178-186.

- [8] M.A.A. Mendes, P. Talukdar, S. Ray, D. Trimis, Detailed and simplified models for evaluation of effective thermal conductivity of open-cell porous foams at high temperatures in presence of thermal radiation, *International Journal of Heat and Mass Transfer* 68 (2013) 612-624.
- [9] B. Rousseau, M. Michiel, A. Canizares, D. De Sousa Meneses, P. Echegut, J.-F. Thovert, Temperature effect (300-1500K) on the infrared photon transport inside an x-ray microtomographic reconstructed porous silica glass, *Journal of Quantitative Spectroscopy and Radiative Transfer* 104 (2007) 257-265.
- [10] S. Haussener, P. Coray, W. Linpinski, P. Wyss, A. Steinfeld, Tomography-based heat and mass transfer characterization of reticulate porous ceramics for high-temperature processing, *ASME Journal of Heat Transfer* 132 (2010) 023305.
- [11] J. Petrasch, S. Haussener, W. Lipinsky, Discrete vs. continuum-scale simulation of radiative transfer in semitransparent two-phase media, *Journal of Quantitative Spectroscopy and Radiative Transfer* 112 (2011) 1450-1459.
- [12] P. Ferkl, R. Pokorny, J. Kosek, Multiphase approach to coupled conduction-radiation heat transfer in reconstructed polymeric foams, *International Journal of Thermal Sciences* 83 (2014) 68-79.
- [13] M. Niezgoda, D. Rochais, F. Enguehard, B. Rousseau, P. Echegut, Modeling heat transfer within porous multiconstituent materials, *Journal of Physics : Conference Series* 369 (2012) 012001.
- [14] P. Boulet, G. Jeandel, G. Morlot, Model of radiative transfer in fibrous media, *International Journal of Heat and Mass Transfer* 38 (1993) 4287-4297.
- [15] D. Le Hardy, M.A. Badri, B. Rousseau, S. Chupin, D. Rochais, Y. Favennec, 3D numerical modelling of the propagation of radiative intensity through a X-ray tomographed ligament, *Journal of Quantitative Spectroscopy and Radiative Transfer* 194 (2017) 86-97.
- [16] M.A. Badri, Y. Favennec, P. Jolivet, B. Rousseau, Conductive-radiative heat transfer within SiC-based cellular ceramics at high temperatures : a discrete scale finite element analysis, *Finite Elements in Analysis and Design* 178 (2020) 103410.
- [17] M.A. Badri, P. Jolivet, B. Rousseau, Y. Favennec, High performance computation of radiative transfer equation using the finite element method, *Journal of Computational Physics* 360 (2018) 74-92.
- [18] T. Fiedler, I.V. Belova, A. Öchsner, G.E. Murch, Non-linear calculations of transient thermal conduction in composite materials, *Computational Materials Science* 45 (2009) 434-438.

- [19] I.V. Belova, G.E. Murch, T. Fielder, A. Öchsner, The Lattice Monte Carlo method for solving phenomenological mass and heat transport problems, *Diffusion Fundamentals* 4 (2007) 15.1-15.23.
- [20] G.L. Vignoles, A hybrid random walk method for the simulation of coupled conduction and linearized radiation transfer at local scale in porous media with opaque solid phases, *International Journal of Heat and Mass Transfer* 93 (2015) 707-719.
- [21] Y. Dauvois, Modélisation du transfert thermique couplé conductif et radiatif au sein de milieux fibreux portés à haute température, PhD work, Université Paris Saclay (France), December 2016 (<https://tel.archives-ouvertes.fr/tel-01502882/document> - manuscript written in French).
- [22] G.L. Vignoles, W. Ros, I. Szelengowicz, C. Germain, A brownian motion algorithm for two scale modeling of chemical vapor infiltration, *Computational Materials Science* 50 (2011) 1871-1878.
- [23] T. Fiedler, R. Löffler, T. Bernthaler, R. Winkler, I.V. Belova, G.E. Murch, A. Öchsner, A numerical analysis of the thermal conductivity of random hollow sphere structures, *Materials Letters* 63 (2008) 1125-1127.
- [24] M. Grigoriu, Local solutions of Laplace, heat and other equations by Itô processes, *Journal of Engineering Mechanics* 123 (1997) 823-829.
- [25] M. Grigoriu, A Monte Carlo solution of heat conduction and Poisson equations, *ASME Journal of Heat Transfer* 122 (2000) 40-45.
- [26] E. Buckingham, On physically similar systems - Illustrations of the use of dimensional equations, *Physical Review* 4 (1914) 345-376.
- [27] R. Herbin, Analyse numérique des équations aux dérivées partielles (document written in French), lecture of the Aix-Marseille University, Marseille (France), 2011, <https://cel.archives-ouvertes.fr/cel-00637008>.
- [28] A. Singer, Z. Schuss, B. Nadler, Unidirectional flux in brownian and Langevin simulations of diffusion, *AIP Conference Proceedings* 800, 400 (2005).
- [29] W.J. Parker, R.J. Jenkins, C.R. Butler, G.L. Abbott, Flash method of determining thermal diffusivity, heat capacity and thermal conductivity, *Journal of Applied Physics* 32 (1961) 1679-1684.
- [30] E.E. Rassy, Y. Billaud, D. Saury, Simultaneous and direct identification of thermophysical properties for orthotropic materials, *Measurement* 135 (2019) 199-212.
- [31] E.E. Rassy, Y. Billaud, D. Saury, Unconventional flash technique for the identification of multilayer thermal diffusivity tensors, *International Journal of Thermal Sciences* 155 (2020) 106430.

- [32] S. André, A. Degiovanni, A theoretical study of the transient coupled conduction and radiation heat transfer in glass: phonic diffusivity measurements by the flash technique, *International Journal of Heat and Mass Transfer* 38 (1995) 3401-3412.
- [33] M. Lazard, S. André, D. Maillat, D. Baillis, A. Degiovanni, Flash experiment on a semitransparent material: interest of a reduced model, *Inverse Problems in Engineering* 9 (2007) 413-429.
- [34] R. Coquard, J. Randrianalisoa, S. Lallich, D. Baillis, Extension of the flash method to semitransparent polymer foams, *ASME Journal of Heat Transfer* 133 (2011) 112604.
- [35] R. Coquard, D. Rochais, D. Baillis, Experimental investigations of the coupled conductive and radiative heat transfer in metallic/ceramic foams, *International Journal of Heat and Mass Transfer* 52 (2009) 4907-4918.

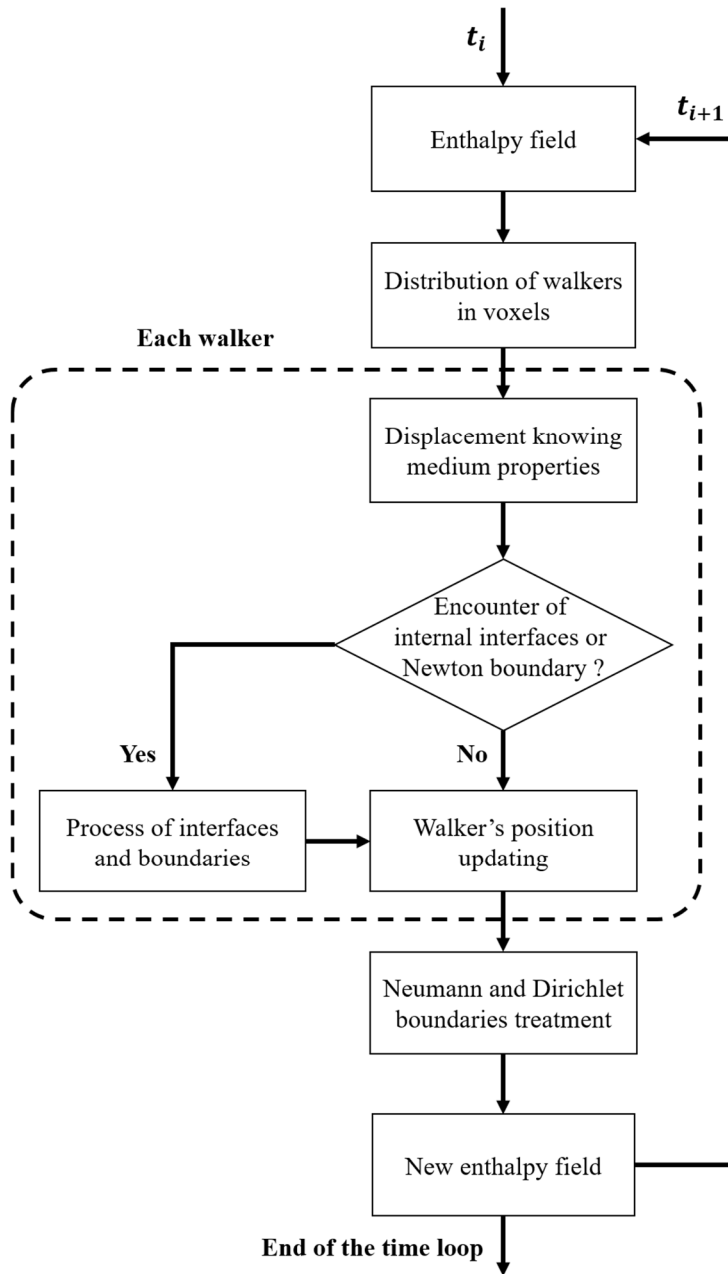


Figure 1: Flowchart of a typical walker calculation.

This figure may be printed in grey.

Single column fitting image.

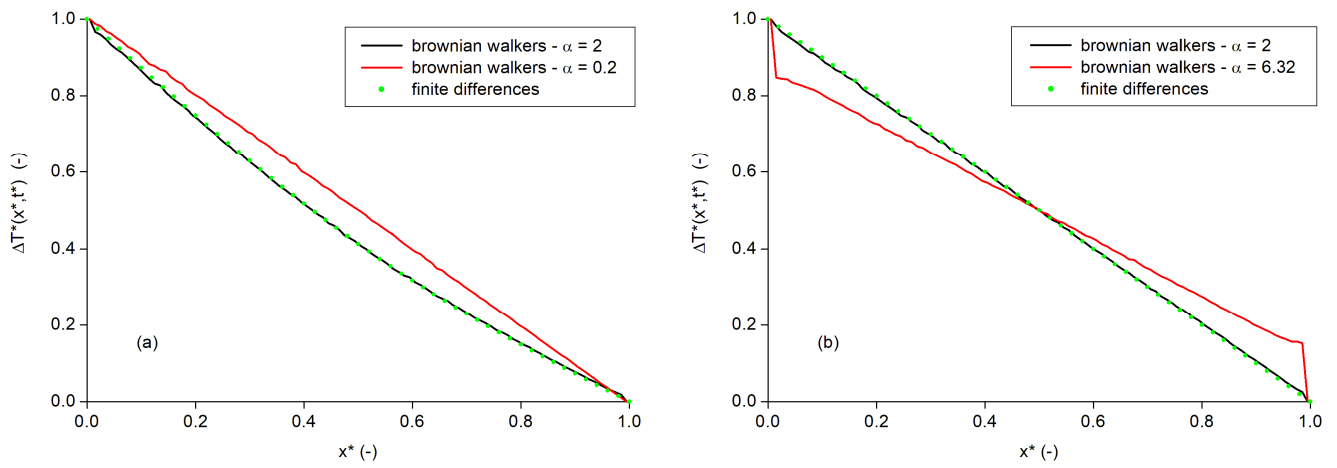


Figure 2: Study of the influence of the time step of the Brownian walker model. Figure 2(a): Temperature elevation profiles ΔT^* at instant $t^* = 0.2$ (transient state) following a decrease of δt^* . Figure 2(b): Temperature elevation profiles ΔT^* at instant $t^* = 2$ (asymptotic steady state) following an increase of δt^* .

*This figure should be printed in colour.
 Two column fitting image.*

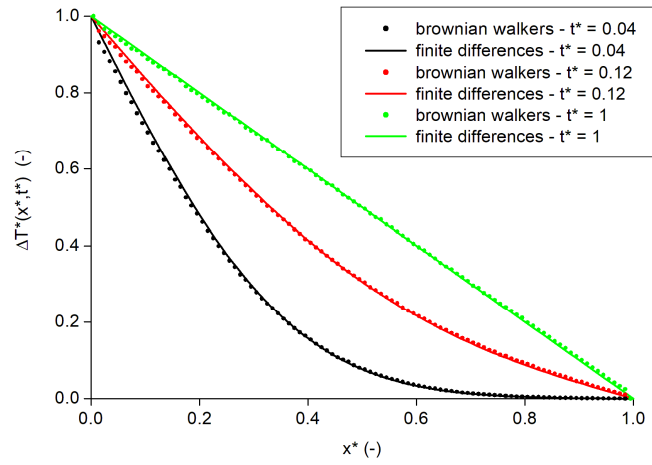


Figure 3: Temperature elevation profiles ΔT^* at different instants t^* in a homogeneous 1D medium subjected to two imposed temperatures. Discrete markers = Brownian walkers; continuous curves = finite differences.

This figure should be printed in colour.

Single column fitting image.

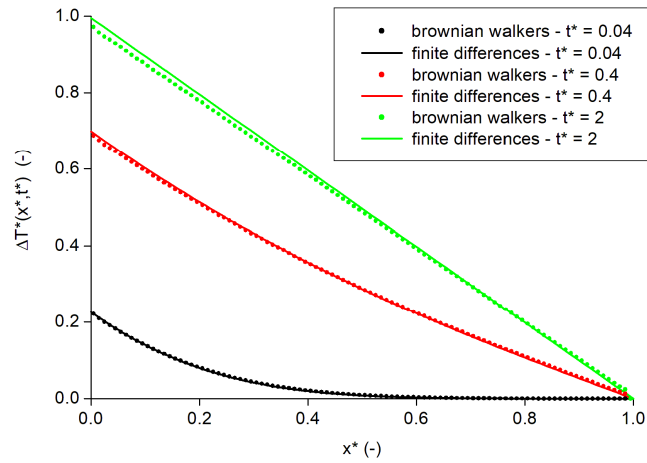


Figure 4: Temperature elevation profiles ΔT^* at different instants t^* in the case of an imposed flux at the front face and an imposed temperature at the rear face. Discrete markers = Brownian walkers; continuous curves = finite differences.

This figure should be printed in colour.

Single column fitting image.

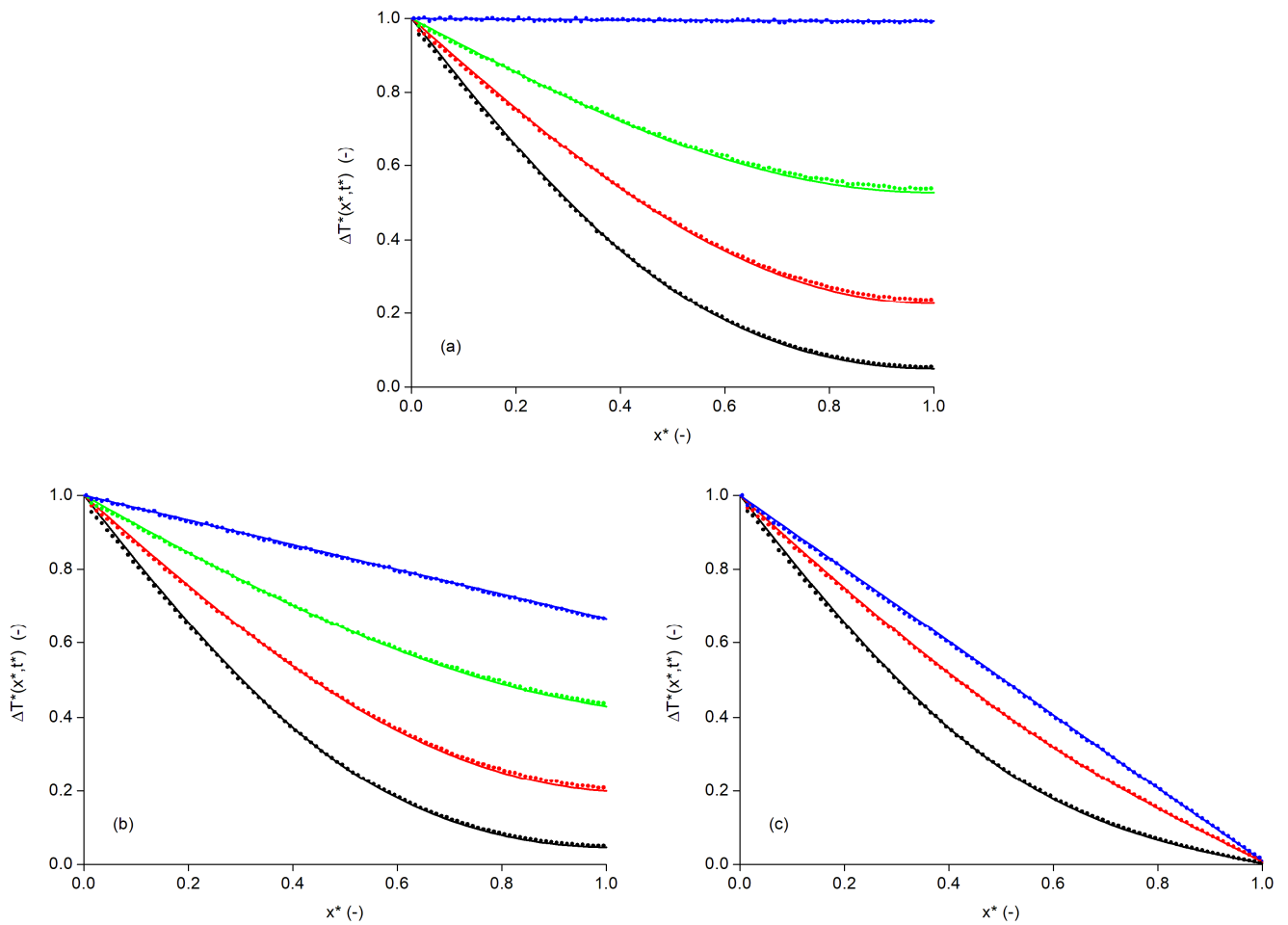


Figure 5: Temperature elevation profiles ΔT^* at different instants (black: $t^* = 0.1$; red: $t^* = 0.2$; green: $t^* = 0.4$; blue: $t^* = 2$) in the case of a face subjected to convective heat losses. Figure 5(a): $Bi = 0$; Figure 5(b): $Bi = 0.5$; Figure 5(c): $Bi = 100$. Discrete markers = Brownian walkers; continuous curves = finite differences.

This figure should be printed in colour.

Two column fitting image.

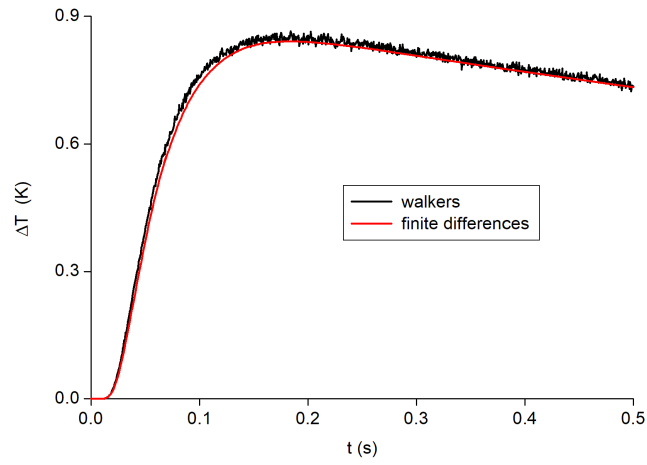


Figure 6: Rear face flash thermograms obtained by walkers (black curve) and by finite differences (red curve).

This figure should be printed in colour.

Single column fitting image.

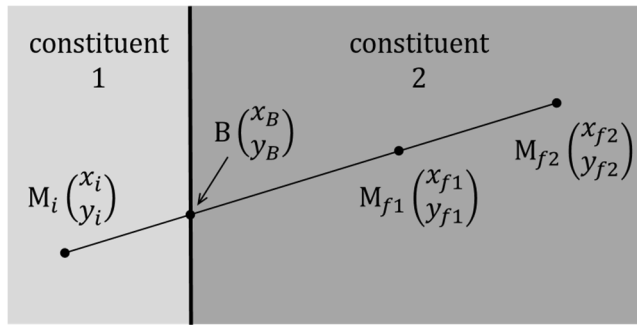


Figure 7: Final position of a walker crossing the interface of two constituents of a heterogeneous medium. In the case illustrated here, $a_2 > a_1$.

This figure may be printed in grey.

Single column fitting image.

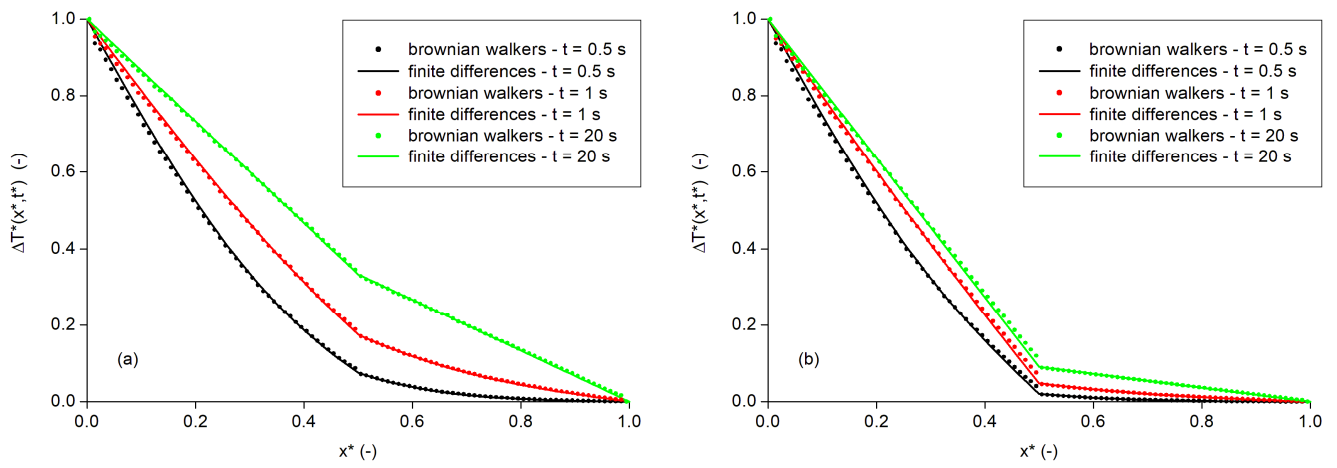


Figure 8: Comparison of the temperature elevation profiles obtained by Brownian walkers (discrete markers) and by finite differences (continuous curves) in a bilayer medium having an effusivity contrast equal to 2 (Figure 8(a)) and equal to 10 (Figure 8(b)).

This figure should be printed in colour.

Two column fitting image.

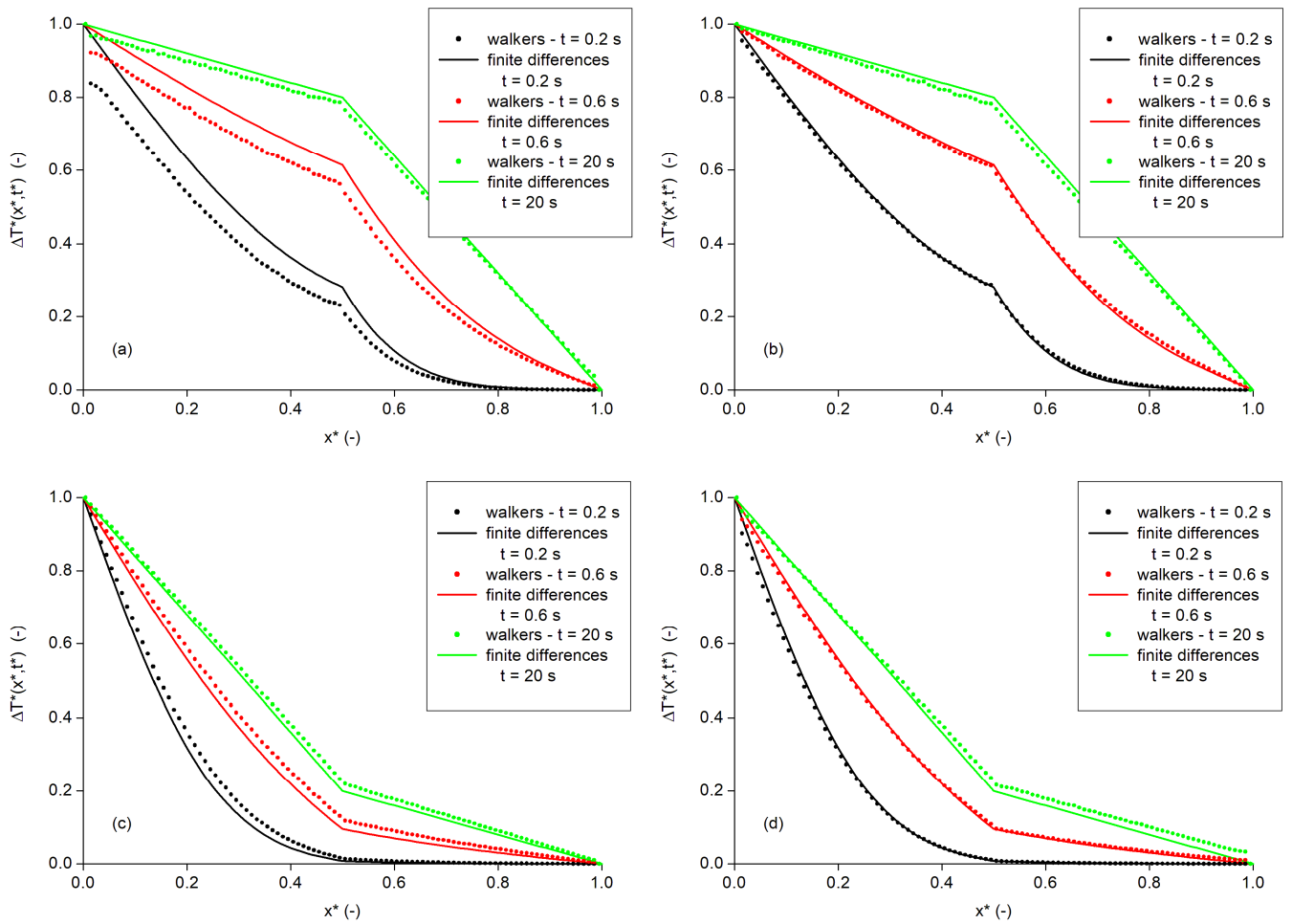


Figure 9: Comparison of the temperature elevation profiles obtained by Brownian walkers (discrete markers) and by finite differences (continuous curves) in a bilayer medium having an effusivity contrast equal to 2 and a diffusivity contrast equal to 4. The cases treated differ by the positions of the two materials in the bilayer and by the material taken for reference in the calculation of the time step.

This figure should be printed in colour.

Two column fitting image.

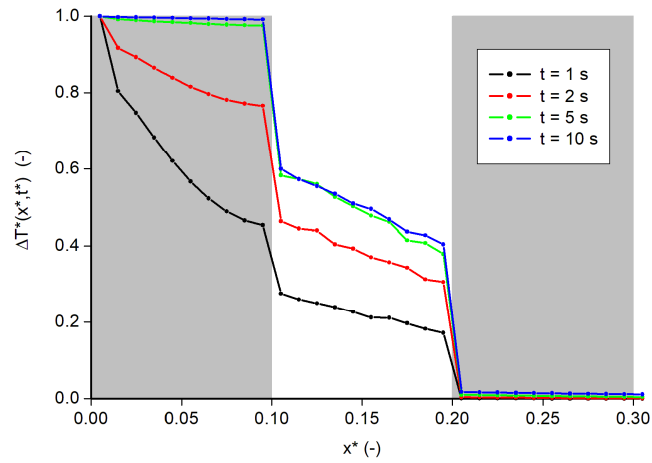


Figure 10: Enlargements over the domain $0 \leq x^* \leq 0.3$ of the temperature elevation profiles calculated by Brownian walkers at different instants of the transient state in a ZrO_2 / air multilayer sample subjected to two imposed temperature conditions. Grey zones = ZrO_2 ; white zone = air.

This figure should be printed in colour.

Single column fitting image.

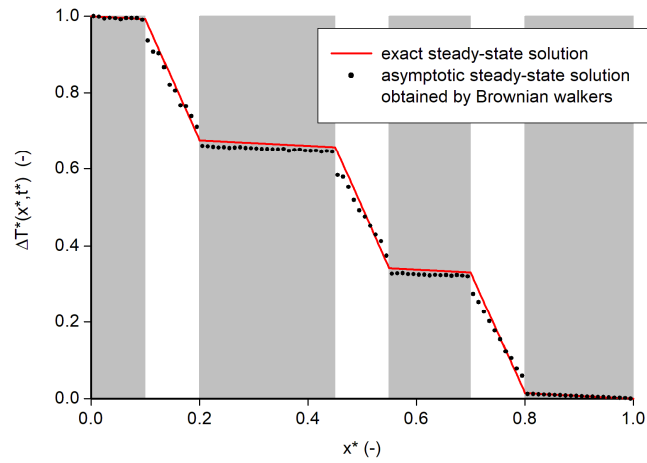


Figure 11: Comparison of the temperature elevation profiles in a ZrO_2 / air multilayer sample. The result with Brownian walkers was obtained after modification of the product ρC_p of air in order to equalize the thermal diffusivities of air and ZrO_2 . Grey zones = ZrO_2 ; white zones = air.

This figure should be printed in colour.

Single column fitting image.